Evaluation of the OSC-TV Reconstruction Algorithm for Optical Cone-Beam Computed Tomography

D. Matenine[1], Y. Goussard[2] and P. Després[1,3]

[1] Département de physique, de génie physique et d'optique, Université Laval, Québec (Québec), Canada
[2] Département de génie électrique / Institut de génie biomédical, École Polytechnique de Montréal, Montréal (Québec), Canada
3 Département de radio-oncologie, CHU de Québec, Québec (Québec), Canada

Abstract— **This paper evaluates an iterative reconstruction technique, the OSC-TV regularized maximum-likelihood algorithm, in the field of optical cone-beam computed tomography (CT). This imaging modality is commonly used in gel-based three-dimensional (3D) dosimetry for external beam radiotherapy. It is conjectured that model-based iterative reconstruction may improve optical CT image quality and encourage a wider use of this modality in clinical dosimetry. The OSC-TV algorithm was evaluated using experimental data from a commercially available optical cone-beam CT system, and the resulting images were compared with those obtained via filtered backprojection. Physical phantoms were scanned with the goal of evaluating the modulation transfer function, reconstruction precision and accuracy. Reconstruction artifacts were studied as well. The OSC-TV algorithm yielded images of improved quality compared to the filtered backprojections, thanks to a model-based simulation of the photon attenuation process. It was shown to improve spatial resolution, reduce noise and improve accuracy and precision of linear attenuation coefficients' estimation. In addition, image artifacts due to acquisition process and total signal loss were corrected. Overall, this study demonstrates that OSC-TV represents a valuable alternative to filtered backprojection for optical cone-beam CT.**

Keywords— **Optical CT, cone-beam CT, iterative reconstruction, total variation minimization**

I. Introduction

Optical computed tomography is a 3D imaging technique used to estimate the distribution of linear attenuation coefficients in optically attenuating objects. One of the applications of optical CT is the reading of dosimetric gels used in external beam radiotherapy. In recent years, the development of complex highly conformal treatment techniques, such as intensity modulated radiotherapy (IMRT) and stereotactic radiosurgery, created a demand for 3D dosimetric tools [1, 2], such as radiosensitive gels. These tools are expected to be convenient and reliable when commissioning new treatment delivery techniques and performing quality assurance procedures. However, gel dosimetry requires complex lab manipulations. The gold standard for gel reading is magnetic resonance imaging (MRI) – a relatively long and expensive procedure. Optical CT represents an interesting alternative to MRI reading. Many apparatus designs may be found in the literature [1, 3], but few are commercially available. The scanner type of interest in this paper is cone-beam optical CT. It is characterized by very short scan times and a simple low-cost design, at the expense of lower image accuracy when compared to sophisticated designs. However, advanced reconstruction algorithms may alleviate this drawback.

Current optical CT systems mostly rely on filtered backprojection to reconstruct 3D images [4, 5]. In particular, the Feldkamp-Davis-Kress (FDK) [6] approach is applied to cone-beam projection data. Such algorithms are not based on a physical model of the photon attenuation process and introduce artifacts even using high-quality acquisitions. Recently, Rankine and Oldham [7], as well as Doran and Yatigammana [8] applied iterative reconstruction to optical CT, in both cases using only simulated parallel-beam projections on a 2D reconstruction grid. In both papers, iterative reconstruction resulted in improved images at the cost of long computation times. In light of these results, additional properties of iterative reconstruction in optical CT still have to be further investigated. Therefore, the current paper used experimental data reconstructed on a 3D grid, and image quality as well as reconstruction times were assessed. A robust iterative algorithm known as the OSC-TV [9], which has shown interesting artifact-reducing properties in X-ray CT, was used in this work. It is characterized by a Poisson log-likelihood objective function, using expectation-maximization to reach the optimum. Regularization is performed via total variation (TV) minimization [10].

II. Materials and Methods

A. Forward model

In optical CT, the basic physical setup consists of a light source, an attenuating object and a detector. The data acquisition results in readings of visible light exposure after propagation in the partially attenuating medium. A set of detector readings acquired in a particular geometric configu-

D.A. Jaffray (ed.), *World Congress on Medical Physics and Biomedical Engineering, June 7-12, 2015, Toronto, Canada*,
IFMBE Proceedings 51, DOI: 10.1007/978-3-319-19387-8_57

ration is called a projection. A set of 2D projections acquired at different light incidence angles is a projection dataset. To solve the inverse problem of 3D image reconstruction from projections, a forward model was first selected – the discretized Beer-Lambert law for monochromatic electromagnetic waves:

$$Y_i = d_i \exp\left[-\sum_j l_{ij}\mu_j\right], \quad (1)$$

where i denotes the reading index, and j – the crossed voxel index. Y denotes the array of detector readings, d – the corresponding non-attenuated readings, l are discrete distance elements in the crossed voxels and μ are the voxels' linear attenuation coefficients. This simple model fits well the physics involved in optical CT and is also often used in X-ray CT. In this work, the light source has a narrow emission spectrum, see Sec. II.C, so the monochromatic approximation is valid. Moreover, it allows one to assume that the detector is a photon counter, as modeled by the reconstruction algorithm, see next section. It is assumed that photons follow straight lines from source to detector, which is an approximation, considering possible refraction at optical interfaces and photon scatter in turbid materials.

B. OSC-TV algorithm

Iterative reconstruction has been shown to improve image quality in X-ray CT [11] and is expected to behave similarly in optical CT, considering the similar forward models. Here, OSC-TV has been selected considering its artifact-reducing properties and use of very few free parameters. It assumes that detector readings follow a Poisson distribution, which properly models low-photon counts, reducing streaking artifacts. The objective function originates from the *convex* algorithm and the optimization is performed via ordered-subsets convex (OSC) expectation-maximization [12]. The distance elements for the forward and inverse models are obtained via the Siddon's method [13]. Regularization is performed after each OSC iteration, using 3D total variation minimization via gradient descent [10], known to reduce high-frequency noise. The OSC algorithm is modified in order to accommodate TV regularization, using gradual subset number reduction [9]. OSC-TV is computationally intensive and was implemented on graphics hardware (GPU) using the CUDA architecture [14] to yield execution times of one to two minutes.

C. Phantoms and optical cone beam scanner

This study used a commercially available cone-beam optical scanner and several optical phantoms designed to assess image quality. They are all part of the DeskCAT™ educational system, manufactured by Modus Medical Devices Inc. (London, ON, Canada). The phantoms consisted of clear plastic jars filled with different materials. The first phantom contained uniformly dyed water to assess the μ estimation accuracy and precision. The second jar contained two gels of different μ values, forming a sharp edge, see Fig. 1 (a), to compute the system modulation transfer function (MTF) and evaluate spatial resolution. The third jar was filled with air and contained a clear plastic sheet with printed opaque line patterns, to evaluate signal loss artifacts. A jar containing a mouse-shaped object formed by gels of different μ values, was used to visualize streaking in 3D.

The DeskCAT scanner, see Fig. 1 (b, c), was used to perform acquisitions. It was designed to closely mimic an X-ray cone-beam axial scanner for the purpose of radiology professionals' training. However, the waves' propagation direction is reversed. The scanner is equipped with a diffuse light source panel illuminated by narrow emission spectrum LEDs, mimicking a flat-panel detector. The light crosses a liquid-filled tank which ensures minimal light refraction. The liquid's refractive index n is closely matched to the phantom's n. A phantom is submerged in the tank and is rotated to acquire several projections. The light is captured by a video camera, its' focal point mimicking a point X-ray source. Before acquiring a projection dataset Y, a calibration scan d is acquired using a transparent phantom. This design provides many advantages: low production costs, short scan times and simple calibration. It also has notable drawbacks: the refraction is not totally eliminated at the gel jar wall,

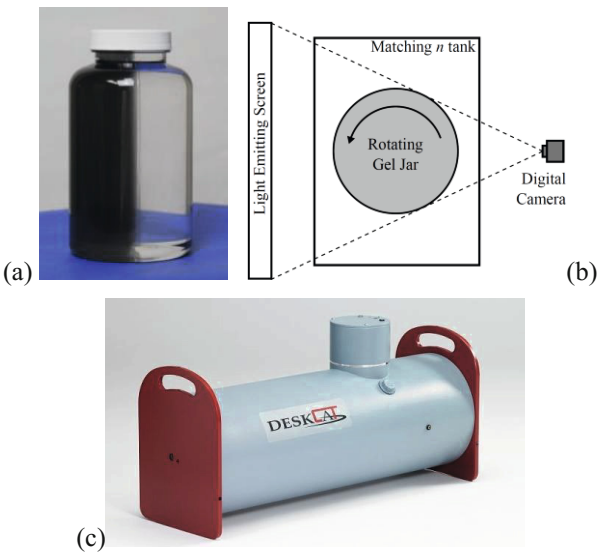

Fig. 1 (a) Typical gel jar, edge phantom shown. (b) Simplified diagram of a cone-beam optical CT scanner. (c) External view of the DeskCAT scanner. Images (a), (c) provided by Modus Medical Devices Inc.

creating boundary artifacts. Convection currents provoke local n variations, inducing artifacts similar to high-frequency noise [3]. Moving debris in suspension create undesired attenuation, yielding similar artifacts. Considering these factors, we conjecture that a regularized iterative reconstruction can improve image quality using *a priori* knowledge about the scanning system and image properties.

D. Acquisition and reconstruction parameters

The datasets consisted of 400 projections each. The camera resolution was of 640×480 pixels. The physical distance from the system isocenter to the camera chip was about 40 cm. The light source was situated at 4.5 cm from the isocenter. For the first three phantoms' reconstructions, the slice resolution was set to 320×320 cubic voxels with 0.25 mm sides, while the mouse-like phantom was reconstructed using 320×240 projections, resulting in slices of 160×160 voxels with 0.5 mm sides. The reference FDK reconstructions used a ramp filter multiplied by a Hamming window. The current implementation of OSC-TV can reconstruct FOVs of limited size due to large memory requirements [9]. Thus, the axial or z-span of the first three volumes is about 64 slices, and 106 slices for the mouse. The OSC-TV reconstruction times per dataset were of about 100 seconds using an NVIDIA® Titan™ GPU. The reference FDK reconstructions were obtained using an in-house code on an Intel® Core™ i7 CPU (single core used) and required times of roughly seven minutes.

III. Results

The uniform phantom was used to assess reconstruction accuracy. Knowing the phantom geometry, the μ value of the uniform phantom was estimated without recurring to CT reconstruction: based on 1600 detector readings, it was determined as (0.235 ± 0.004) cm^{-1}. A circular region of interest (ROI) was analyzed at the central slice of reconstructed images, covering 48% of the jar cross-section. OSC-TV outputs images directly as μ coefficients and yielded roughly the same result: (0.233 ± 0.005) cm^{-1}. In contrast, FDK output needed normalization, and a scaling constant was found using a least-squares fit on projection data. The FDK result was (0.26 ± 0.03) cm^{-1}, less accurate and less precise than the result of OSC-TV.

The edge phantom scan was reconstructed using FDK and OSC-TV. The central slice is shown in Fig. 2. The μ interval is set to [0.0, 0.5] cm^{-1}, corresponding to the plateau values of the phantom. The FDK result shows concentric ring artifacts. OSC-TV produces a more uniform image. The outmost ring, due to refraction at the gel jar wall, is still visible, but less prominent than in the FDK image.

In order to compare spatial resolution, the edge response function (ERF) was sampled for the FDK and OSC-TV images, at the central slice. The profile was acquired perpendicularly to the visible edge, at a distance of a half-radius of the imaged jar from the isocenter, with a sampling width of 3 voxels. The raw profiles were fitted to a Gauss error function. The resulting MTFs are shown in Fig. 3, and OSC-TV yields a better resolution. In order to validate these findings, the noise level was measured in these images, in ROIs of 32×32 voxels known to be uniform in the phantom, and OSC-TV yielded roughly six to eight times lower noise standard deviation than FDK. Overall, OSC-TV simultaneously provides increased spatial resolution and lower noise.

The opaque line pair phantom was used to assess the artifacts arising from total signal loss at the detector. Fig. 4 shows reconstructed slices containing a single opaque line. FDK features streaking, prominent halos around the line and *black holes* of negative μ at the ends of the line. With OSC-TV, the black holes are suppressed, while streaking and halos are reduced. These results are consistent with the better modeling of the attenuation process by OSC-TV. Similarly, the mouse-like phantom contained several heavi-

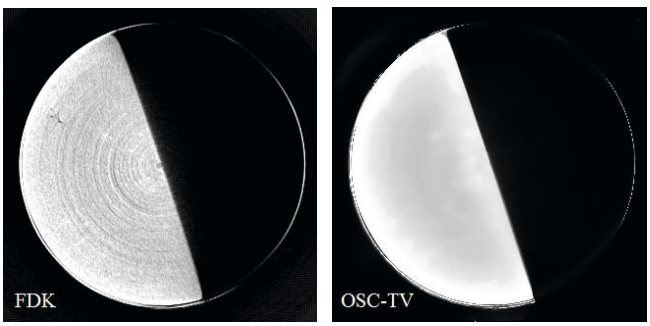

Fig. 2 Central slice of the edge phantom. The μ interval is [0.0, 0.5] cm^{-1}. Note the ring artifacts for FDK and a more uniform result for OSC-TV.

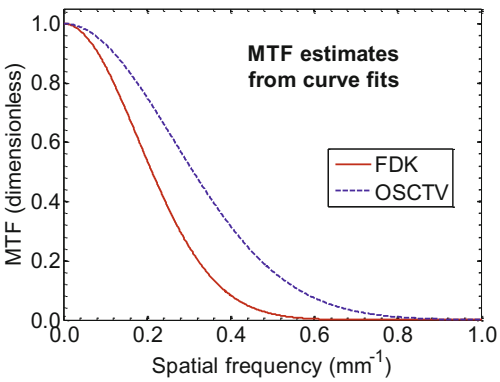

Fig. 3 MTF estimates obtained from the edge profiles' fits. Note the higher spatial resolution for OSC-TV.

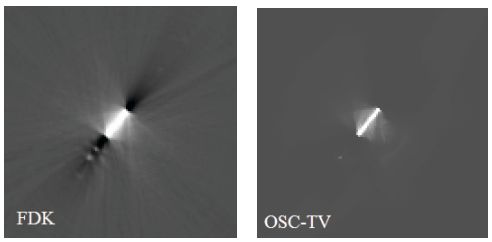

Fig. 4 Opaque line images, ROI of 128×128, the μ interval is [-3, 5] cm^{-1}.

ly attenuating structures, causing streaking in FDK images, yet not affecting OSC-TV. As shown in Fig. 5, the "cloudy" areas around the mouse "neck" result from streaking.

IV. Discussion

Compared to the FDK algorithm, OSC-TV demonstrated interesting properties. However, it is acknowledged that the phantoms used in this study were quite simple. They did not contain complex μ gradients or objects of small physical size and/or low contrast. Nevertheless, this approach seems relatively well-suited for gel dosimetry, where dose distributions are often composed of large uniform regions.

V. Conclusion

This paper presented a comparative evaluation of 3D reconstructions obtained via the iterative OSC-TV and FDK algorithms in optical cone-beam CT. The results are based on experimental projection data acquired from physical phantoms' scans. OSC-TV was shown to offer better spatial resolution, lower noise, better μ accuracy and precision, as well as to reduce artifacts such as streaking. Refraction artifacts are not eliminated, but are attenuated by OSC-TV. Future work is oriented towards a more sophisticated regularization method, as well as the evaluation of the algorithm's performance on realistic gel dosimeters.

Acknowledgment

The authors acknowledge partial support by Fonds de recherche du Québec – Nature et technologies (FRQ-NT) and the CREATE Medical Physics Research Training Network grant of the Natural Sciences and Engineering Research Council of Canada (Grant number: 432290). They also thank John Miller and Jen Dietrich from Modus Medical Devices Inc. for the advice on the DeskCAT system specifications, and Julia Mascolo-Fortin for in-lab assistance.

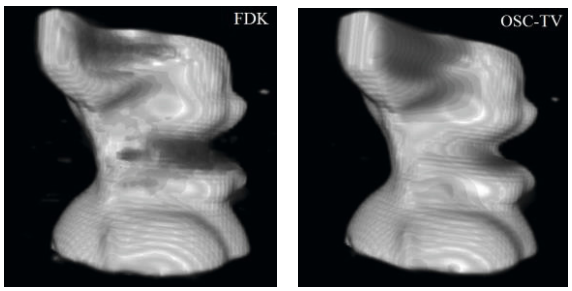

Fig. 5 Volume rendering of the mouse phantom, FDK shows streaking.

References

1. Oldham M, Siewerdsen J H, Kumar S et al. (2003) Optical-CT gel-dosimetry I: Basic investigations Med Phys 30 4:623–634
2. Schreiner L J (2009) Where does gel dosimetry fit in the clinic? J Phys: Conf Ser 164 1:012001
3. Jordan K (2004) Advances in optical CT scanning for gel dosimetry J Phys: Conf Ser 3 1:115–121
4. Krstajic N, Doran S J (2007) Characterization of a parallel-beam CCD optical-CT apparatus for 3D radiation dosimetry Phys Med Biol 52 13:3693–3713
5. Olding T, Holmes O, Schreiner L J (2010) Cone beam optical computed tomography for gel dosimetry I: Scanner characterization Phys Med Biol 55 10:2819–2840
6. Feldkamp L A, Davis L C, Kress J W (1984) Practical cone-beam algorithm J Opt Soc Am (A) 1 6:612–619
7. Rankine L, Oldham M (2013) On the feasibility of optical-CT imaging in media of different refractive index Med Phys 40 5: 051701
8. Doran S J, Yatigammana D N B (2012) Eliminating the need for refractive index matching in optical CT scanners for radiotherapy dosimetry: I. Concept and simulations Phys Med Biol 57 3:665–683
9. Matenine D, Hissoiny S, Després P (2011) GPU-accelerated few-view CT reconstruction using the OSC and TV techniques Proc. Int. Meeting on Fully 3D Image Reconstr. in Rad. and Nucl. Med., Potsdam, Germany, pp 76–79
10. Sidky E Y, Kao C M, Pan X (2006) Accurate image reconstruction from few-views and limited-angle data in divergent-beam CT J XRay Sci Tech 14 2:119–139
11. Pan X, Sidky E Y, Vannier M (2009) Why do commercial CT scanners still employ traditional, filtered back-projection for image reconstruction? Inverse Probl 25 12:123009
12. Beekman F J, Kamphuis C (2001) Ordered subset reconstruction for x-ray CT Phys Med Biol 46 7:1835–1844
13. Siddon R L (1985) Fast calculation of the exact radiological path length for a three-dimension CT array Med Phys 12 2:252–255
14. NVIDIA Corporation Inc., Santa Clara CA (2010) NVIDIA CUDA Reference Manual Version 3.1

Author: Dmitri Matenine
Institute: Université Laval
Street: 1045 av. de la Médecine
City: Québec (QC)
Country: Canada
Email: dmitri.matenine.1@ulaval.ca